

Effect of the number of defect particles on the structure and dispersion relation of a two-dimensional dust lattice system

Rangyue Zhang(张壤月), Guannan Shi(史冠男), Hanyu Tang(唐瀚宇), Yang Liu(刘阳), Yanhong Liu(刘艳红), and Feng Huang(黄峰)

Citation: Chin. Phys. B, 2022, 31 (**3**): 035204. DOI: 10.1088/1674-1056/ac306d
Journal homepage: http://cpb.iphy.ac.cn; http://iopscience.iop.org/cpb

What follows is a list of articles you may be interested in

Long-time evolution of charged grains in plasma under harmonic external force and after being withdrawn

Miao Guan(管苗), Zhi-Dong Chen(陈志东), Meng-Die Li(李梦蝶), Zhong-Mao Liu(刘忠茂), You-Mei Wang(汪友梅), and Ming-Yang Yu(郁明阳)
Chin. Phys. B, 2022, 31 (**2**): 025201. DOI: 10.1088/1674-1056/ac0e27

Attenuation characteristics of obliquely incident electromagnetic wave in weakly ionized dusty plasma based on modified Bhatnagar-Gross-Krook collision model

Zhaoying Wang(王召迎), Lixin Guo(郭立新), and Jiangting Li(李江挺)
Chin. Phys. B, 2021, 30 (**4**): 045203. DOI: 10.1088/1674-1056/abe230

Directional motion of dust particles at different gear structuresin a plasma

Chao-Xing Dai(戴超星), Chao Song(宋超), Zhi-Xiang Zhou(周志向), Wen-Tao Sun(孙文涛), Zhi-Qiang Guo(郭志强), Fu-Cheng Liu(刘富成), Ya-Feng He(贺亚峰)
Chin. Phys. B, 2020, 29 (**2**): 025203. DOI: 10.1088/1674-1056/ab6109

Electric field in two-dimensional complex plasma crystal: Simulated lattices

Behnam Bahadory
Chin. Phys. B, 2018, 27 (**2**): 025202. DOI: 10.1088/1674-1056/27/2/025202

Analysis of electron energy distribution function in a magnetically filtered complex plasma

M K Deka, H Bailung, N C Adhikary
Chin. Phys. B, 2013, 22 (**4**): 045201. DOI: 10.1088/1674-1056/22/4/045201

Effect of the number of defect particles on the structure and dispersion relation of a two-dimensional dust lattice system

Rangyue Zhang(张壤月)[1], Guannan Shi(史冠男)[2], Hanyu Tang(唐瀚宇)[1], Yang Liu(刘阳)[1], Yanhong Liu(刘艳红)[3], and Feng Huang(黄峰)[1,†]

[1] *College of Science, China Agricultural University, Beijing* 100083, *China*
[2] *College of Information and Electrical Engineering, China Agricultural University, Beijing* 100083, *China*
[3] *School of Physics and Optoelectronic Engineering, Ludong University, Yantai* 264025, *China*

(Received 1 June 2021; revised manuscript received 13 October 2021; accepted manuscript online 18 October 2021)

The effect of the number of defect particles on the structure and dispersion relations of a two-dimensional (2D) dust lattice is studied by molecular dynamics (MD) simulation. The dust lattice structures are characterized by particle distribution, nearest neighbor configuration and pair correlation function. The current autocorrelation function, the dispersion relation and sound speed are used to represent the wave properties. The wave propagation of the dust lattice closely relates to the lattice structure. It shows that the number of defect particles can affect the dust lattice local structure and then affect the dispersion relations of waves propagating in it. The presence of defect particles has a greater effect on the transverse waves than on the longitudinal waves of the dust lattice. The appropriate number of defect particles can weaken the anisotropy property of the lattice.

Keywords: complex plasma, molecular dynamics (MD) simulation, defect particles, dust lattice wave

PACS: 52.27.Lw, 52.65.Yy **DOI:** 10.1088/1674-1056/ac306d

1. Introduction

Dusty plasma allows us to study the basic properties of plasma at the level of "atomic" dynamics and allows the visualization of collective plasma behavior, such as the Coulomb lattice and fluctuations.[1–5] The formation of Coulomb lattice is of great significance to study the structure, dynamic properties and phase transition of condensed matter,[6–9] thus it can be used as an ideal simulation system of a condensed matter system. The propagating waves in a dust lattice can effectively show the structure and properties of the lattice, so more and more attention has been paid to the study of dust lattice waves.[10–15]

In a Coulomb lattice, dust particles with the charge Q through absorbing a certain number of electrons and ions can interact by the shielding Coulomb potential or Yukawa potential $\phi(r) = \frac{Q}{4\pi\varepsilon_0 r}\exp(-\frac{r}{\lambda_D})$, where λ_D is the Debye length.[16–18] When the interaction potential energy of dust particles greatly exceeds their kinetic energy (e.g., the ratio of the interaction potential energy to the kinetic energy exceeds the threshold value $\tau_c = 170$),[19,20] dust lattice can be formed. Dust lattices with different structures such as fcc, bcc and hexagonal have been discovered.[12,21,22] Sun *et al.* investigated the dispersion relationship of dust lattice waves under the external magnetic field.[10] Thomas *et al.* studied the effect of particle-wake interaction on the wave dispersion in a 2D dust lattice.[23] When the defect particles appear in a dust lattice formed by uniform particles, the original ordered structure of the lattice will be influenced or destroyed, thus the wave propagation behavior will be affected accordingly. Defect in a dust lattice can be achieved by using very small amount of defect particles (with obviously larger or smaller charge or mass than normal particles) to replace the normal particles. In Ref. [24], the effect of defect particles on the wave dispersion was investigated in a 1D dust chain, and it is found that the appearing of defect particles with larger charge causes the gap in the dispersion relationship with the gap becoming wider as the increase of defect particle charge. For a 2D dust lattice, the structure and wave properties are different from those of a 1D system. The detailed research on the dispersion relations of a 2D dust lattice with defect particles is needed. In this paper, the structure and dispersion relations in a 2D Yukawa dust lattice system with changing the number of defect particles are investigated by simulation.

2. Method of molecular dynamics simulation

In the 2D molecular dynamics (MD) simulations, the NVT ensemble and the Nose–Hoover thermostat are used to maintain the system temperature at $T = 0.0001$ (in the energy unit). The number of defect particles is denoted by N_D with twice the charge of normal particles. The simulation time step is $0.01\omega_{pd}^{-1}$, where $\omega_{pd} = \sqrt{Q^2/\varepsilon M a^3}$ is the dusty plasma frequency (Q and M are the charge and mass of normal dust particles) and the total simulation runs 6×10^4 steps. The length is normalized by λ_D and the time is normal-

†Corresponding author. E-mail: huangfeng@cau.edu.cn
© 2022 Chinese Physical Society and IOP Publishing Ltd

ized by $t_0 = \sqrt{4\pi\varepsilon_0 M\lambda_D^3/Q^2}$. The dispersion relations of the transverse and longitudinal waves are obtained by the current autocorrelation functions together with the Fourier transformation. The current operator can be expressed as $\boldsymbol{j}(q,t) = \sum_{m=1}^{N} \boldsymbol{v}_m(t)\exp(\mathrm{i}\boldsymbol{q}\cdot\boldsymbol{r}_m(t))$, where $\boldsymbol{v}_m(t)$and $\boldsymbol{r}_m(t)$ are the velocity and the position of the m-th particle at time t, and $\boldsymbol{q} = \boldsymbol{k}a$ is the wave vector. The total particle number N is 400 (including normal and defect particles) in a $L\times L$ box with $L = 20a$ (a is interparticle distance) under a periodical boundary condition. In the simulation, the number of defect particles varied from 1 to 23. When adding defect particles, the initial positions of defect particles with larger charge ($2Q$) were set according to uniformly spatial distribution. As the simulation goes on, the defect particles will move in the particle system, and after the system reaches the equilibrium state, the defect particles will distribute by themselves.

In this paper, the lattice structure is characterized by the pair correlation function, which is defined as

$$g(r) = \frac{S}{N}\cdot\frac{N(r,\Delta)}{2\pi r\Delta}, \tag{1}$$

where S is the area of the simulation region, N is the number of the total dust particles, and $N(r,\Delta)$ indicates the number of dust particles between $r-\frac{\Delta}{2}$ and $r+\frac{\Delta}{2}$ (in this simulation, $\Delta = 0.1a$, where a represents the mean interparticle distance).

The dispersion relations of transverse and longitudinal waves are obtained by calculating the current autocorrelation function and performing the Fourier transformation. The longitudinal and transverse current autocorrelation functions are written as follows:

$$C_{\mathrm{l}}(q,t) = (N)^{-1}\langle[\boldsymbol{q}\cdot\boldsymbol{j}_q(t)][\boldsymbol{q}\cdot\boldsymbol{j}_{-q}(0)]\rangle, \tag{2}$$

$$C_{\mathrm{t}}(q,t) = (2N)^{-1}\langle[\boldsymbol{q}\times\boldsymbol{j}_q(t)]\cdot[\boldsymbol{q}\times\boldsymbol{j}_{-q}(0)]\rangle, \tag{3}$$

where $q = |\boldsymbol{q}| = |\boldsymbol{k}a|$ is the normalized wave number.

The according Fourier transformations are made as follows:[25–27]

$$C_{\mathrm{l,t}}(q,\omega) = \int_0^{\infty}\exp(\mathrm{i}\omega t)C_{\mathrm{l,t}}(q,t)\,\mathrm{d}t. \tag{4}$$

The sound speed can be defined as[28]

$$C_{\mathrm{s}} = \lim_{q\to 0}\frac{\omega(\boldsymbol{q})}{q}. \tag{5}$$

3. Simulation results and discussion

Figure 1(a) shows the distribution of defect particles after the system is in the stable state. The coordinate axis diagram in the lower right corner shows the coordinate system and direction, and θ represents the angle between the wave number and the primitive translation vector (in the x axis direction). To highlight the defect particles, the white points with larger size are used to represent defect particles, while ordinary dust particles are denoted by the white points with normal size. Figure 1(b) shows the nearest neighbor configuration of the system with different defect numbers. As can be seen, when the defect number N_{D} is 1, the system mainly maintains the hexagonal lattice structure. As the number of defect particles increases, the hexagonal lattice structure surrounding the defect particle is destroyed due to the effect of these defect particles. This is in an agreement with the result[29] that particles with different masses and charges have the different thermal equilibrium in a binary system, which can cause the destruction of the ordered structures.

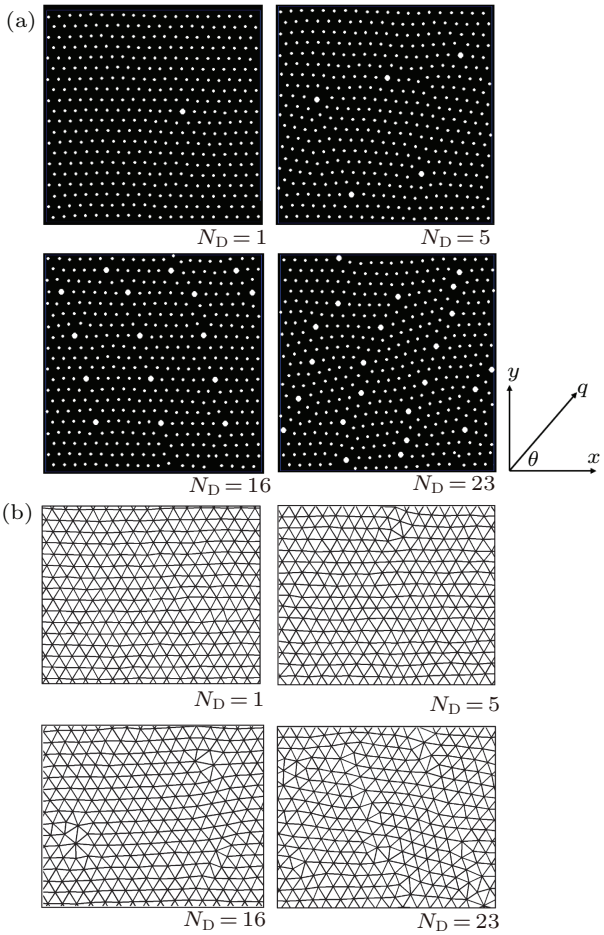


Fig. 1. (a) Distribution of defect particles and (b) the nearest neighbor configuration of particles after the system is in the stable state.

Pair correlation function $g(r)$ is the measurement of the relative probability of finding a particle at a distance r from the reference particle, which can be used to investigate the lattice structure characteristics. Figure 2 shows the $g(r)$ curve of the system and the first peak value $g_{1\mathrm{p}}(r)$ of the $g(r)$ curve changing as the number of defect particles. From Fig. 2(a), it can be seen that with increasing the number of defect particles, the peaks of the $g(r)$ curve gradually become weaken, meaning that the order structure of the dust lattice is weak-

ened. From Fig. 2(a), it can also be seen that the double-peak structure in the second peak of the $g(r)$ curve becomes less and less obvious with the increase of $N_{\rm D}$, indicating that the particle arrangement gradually becomes disordered. From the $g(r)$ curve, the first peak position (shown by the dashed line) and the peak intensity with the different number of defect particles can be obtained. It can be seen that the number of defect particles does not obviously affect the position of the first peak of $g(r)$, but affect the intensity of the first peak. It indicates that a small number of defect particles ($N_{\rm D}$ = 1–23) in the system composed of 400 particles affect the local structure of the system, but from the overall average of the system, the small number of defects does not affect the first peak position of the $g(r)$ curve. The relationship between the first peak intensity $g_{1\rm p}(r)$ and $N_{\rm D}$ is obtained, which is shown in Fig. 2(b). Through the fitting line of $g_{1\rm p}(r)$–$N_{\rm D}$ (in Fig. 2(b)), one can see that with the increase of $N_{\rm D}$, the peak value of $g_{1\rm p}(r)$ significantly decreases, indicating the probability of finding the dust particles at the average interparticle distance from a reference particle gradually decreases as $N_{\rm D}$.

In the 2D hexagonal lattice, longitudinal and transverse waves can propagate in an arbitrary direction, denoted by the angle θ (in Fig. 1(a)). Two independent directions are defined, that is, parallel or horizontal direction ($\theta = 0$) and perpendicular or vertical direction ($\theta = \pi/2$) to primitive translation vector.[30] Figure 3 shows the current autocorrelation functions $C_{\rm l,t}(q,\ \omega)$ of longitudinal and transverse waves in horizontal and vertical directions when the number of defect particles is 0, 7, 16 and 23. From Fig. 3, one can see that the current autocorrelation functions with the number of defect particles of 0 (a1)–(d1), 7 (a2)–(d2), 16 (a3)–(d3) and 23 (a4)–(d4) are mainly different in the case of transverse waves. When $N_{\rm D}$ is 0 and 7, the $C_{\rm l,t}(q,\ \omega)$ with a single peak are dominated in both longitudinal and transverse current autocorrelation functions. However, when $N_{\rm D}$ is increased to 16, it can be seen that the spectra of the transverse current autocorrelation functions (i.e., the $C_{\rm t}(q,\ \omega)$ curves) are significantly more affected by the defect particles than those of longitudinal waves (i.e., the $C_{\rm l}(q,\ \omega)$ curves), that is, the $C_{\rm l}(q,\ \omega)$ curves are still dominated by a single peak, while the $C_{\rm t}(q,\ \omega)$ curves mainly show two separated peaks and some of which are with double peaks. In addition, it can be seen that the peaks in the $C_{\rm l,t}(q,\ \omega)$ curves of $N_{\rm D} = 23$ are more disorder than those of $N_{\rm D} = 16$.

In Fig. 4, the dispersion relations of longitudinal and transverse waves along horizontal and vertical directions with $N_{\rm D}$ being 0, 7 and 16 are shown. It can be seen that for the three $N_{\rm D}$ values the dispersion relations of longitudinal waves in parallel or vertical direction are very close, while for the transverse waves in parallel and vertical direction the dispersion relations show different characteristics. For example, the almost coincident values of ω–q for $N_{\rm D} = 0$ and 7 indicate that the dispersion relation is not greatly affected when the number of defect particles is very small. When $N_{\rm D}$ is 16, the dispersion relations $\omega(t,0)$ and $\omega(t,\pi/2)$ of the transverse waves both in parallel and vertical direction show two branches, with one branch nearly coincident with that of $N_{\rm D} = 0$ and 7 and another branch with higher frequencies. The occurrence of the branch with higher frequencies may be related to the coupling of defect particles participation. It is probably because in this simulation the initially uniformly distributed defect particles with larger charges cause the stronger interaction between defect particles and the surrounding normal particles resulting in the appearance of high frequency collective mode. When the number of defect particles is increased to a certain value, the enhanced collective mode of defect particle participation can be observed in the transverse waves.

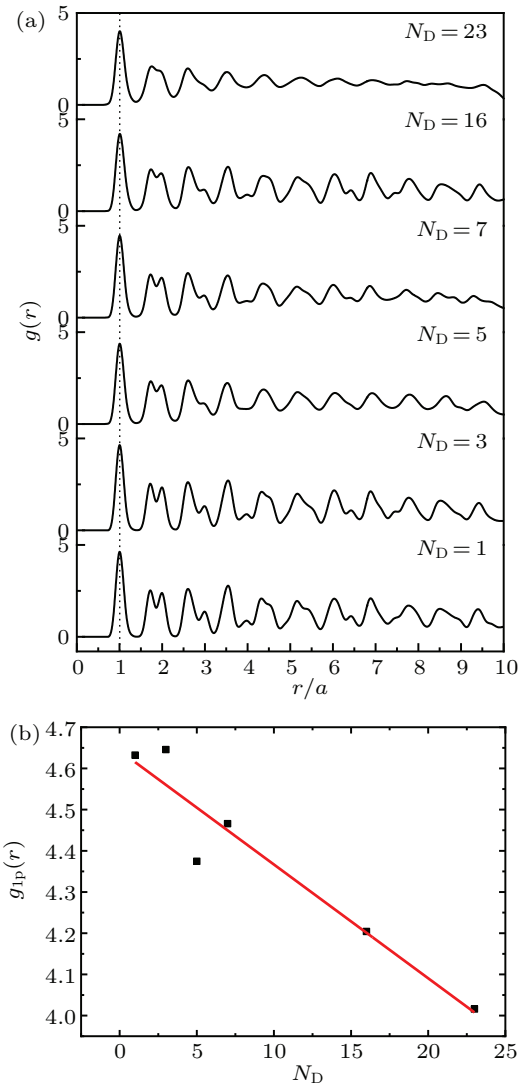
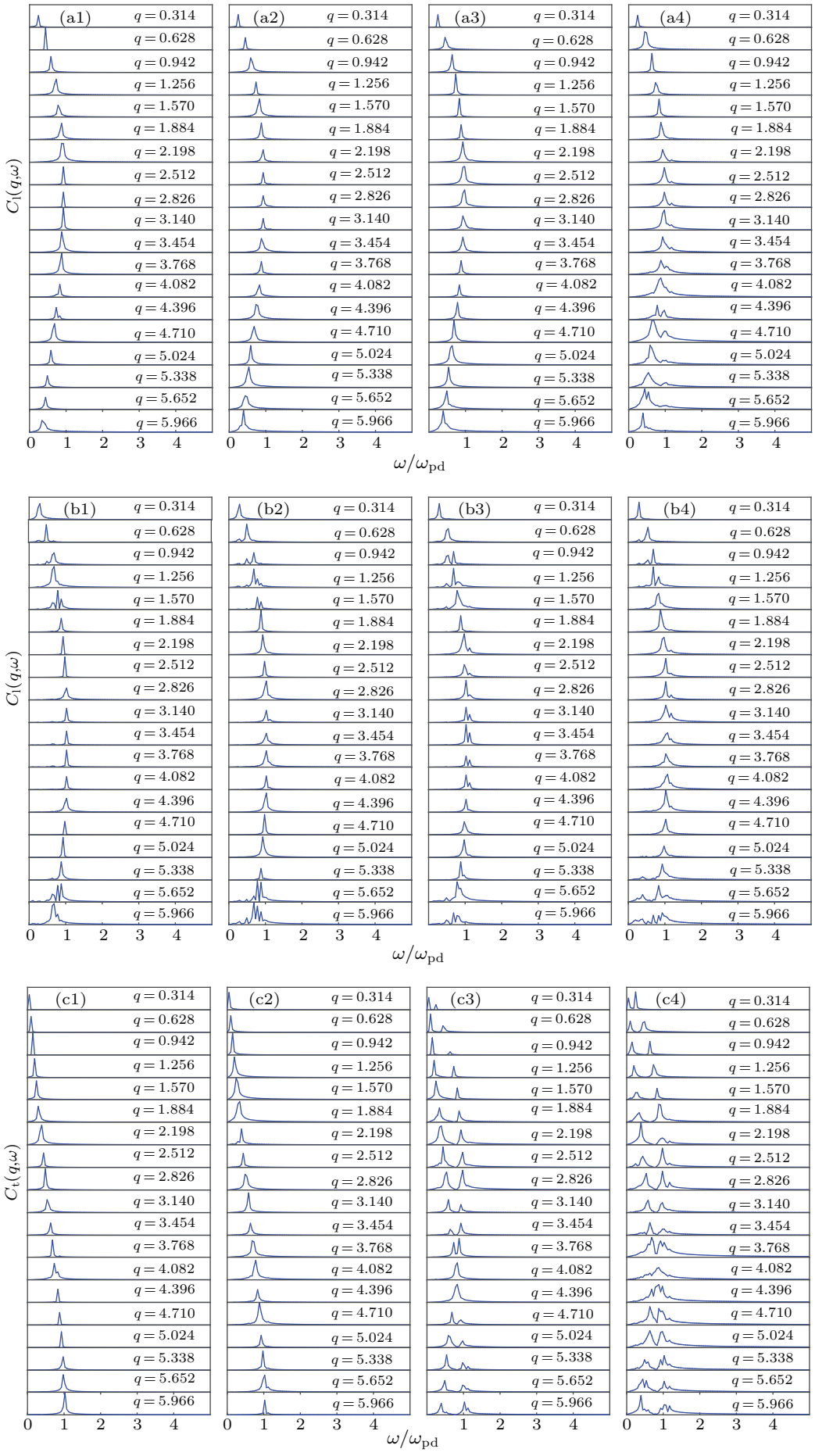


Fig. 2. (a) Pair correlation function $g(r)$ of the system with the different number of defect particles; (b) the relationship between the first peak value of $g(r)$ and the number of defect particles.


(a1)
(a2)
(a3)
(a4)
(b1)
(b2)
(b3)
(b4)
(c1)
(c2)
(c3)
(c4)
$q = 0.314$
$q = 0.628$
$q = 0.942$
$q = 1.256$
$q = 1.570$
$q = 1.884$
$q = 2.198$
$q = 2.512$
$q = 2.826$
$q = 3.140$
$q = 3.454$
$q = 3.768$
$q = 4.082$
$q = 4.396$
$q = 4.710$
$q = 5.024$
$q = 5.338$
$q = 5.652$
$q = 5.966$
$C_{\mathrm{l}}(q,\omega)$
$C_{\mathrm{t}}(q,\omega)$
$\omega/\omega_{\mathrm{pd}}$
0 1 2 3 4

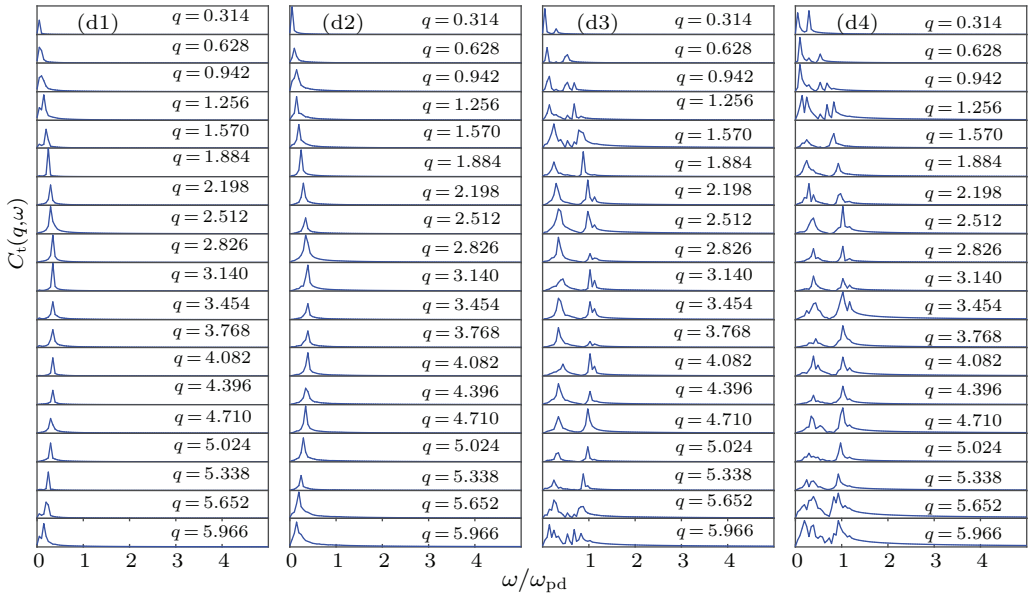


Fig. 3. The wave spectra of the longitudinal and transverse current autocorrelation functions $C_l(q, \omega)$ and $C_t(q, \omega)$ in horizontal ($\theta = 0$) and vertical ($\theta = \pi/2$) directions under different defect numbers, (a1)–(a4) $C_l(q, \omega)$, $\theta = 0$; (b1)–(b4) $C_l(q, \omega)$, $\theta = \pi/2$; (c1)–(c4) $C_t(q, \omega)$, $\theta = 0$; (d1)–(d4) $C_t(q, \omega)$, $\theta = \pi/2$. (a1)–(d1) $N_D = 0$, (a2)–(d2) $N_D = 7$, (a3)–(d3) $N_D = 16$, (a4)–(d4) $N_D = 23$. The waves number q varies from 0.314 to 5.966.

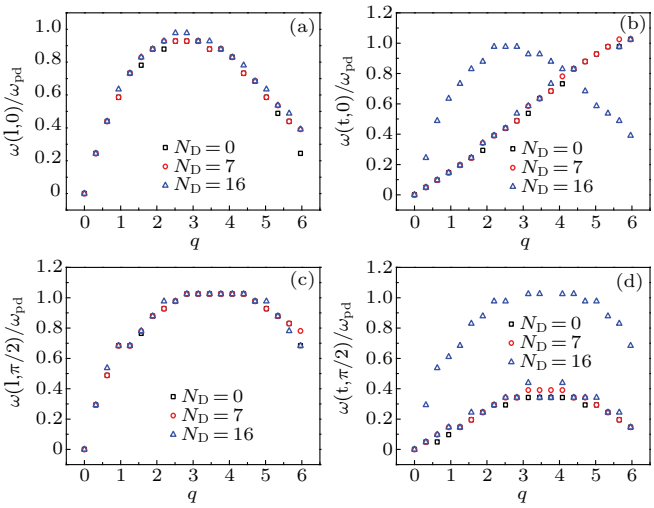


Fig. 4. Dispersion relations of longitudinal and transverse waves in parallel and perpendicular directions under different numbers of defect particles: (a) $\omega(l,0)$, the longitudinal wave along parallel direction ($\theta = 0$); (b) $\omega(t,0)$ the transverse wave in parallel direction; (c) $\omega(l,\pi/2)$, the longitudinal wave along perpendicular direction ($\theta = \pi/2$); (d) $\omega(t,\pi/2)$, the transverse wave along perpendicular direction ($\theta = \pi/2$).

For a more obvious comparison, the dispersion relations of longitudinal and transverse waves with $N_D = 16$ are shown in Fig. 5. It shows that in parallel direction the higher frequency branch of the transverse wave $\omega(t,0)$ almost coincides with the longitudinal wave $\omega(l,0)$. The similar feature was also found in the perpendicular direction, that is, the higher frequency branch of the transverse wave $\omega(t,\pi/2)$ almost coincides with the longitudinal wave $\omega(l,\pi/2)$. It shows that the appearance of the branches of higher frequencies reduces the difference of dispersion relation of waves in different directions. That is, appropriately adding defect particles can weaken the anisotropy of such a hexagonal lattice.

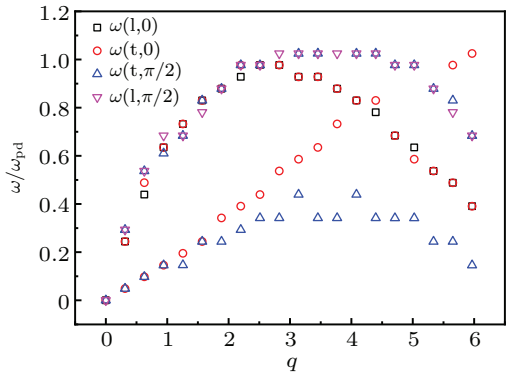


Fig. 5. Dispersion relations of the longitudinal and transverse waves with $N_D = 16$ in parallel and perpendicular directions.

The sound speeds C_s of the longitudinal and transverse waves are also calculated from the dispersion relations in the limit $q \to 0$.[30,31] From the calculation ($N_D = 0$–16), it is known that for the dust lattice without defect particle, the sound speeds of the longitudinal waves are obviously larger than those of the transverse waves, and meanwhile when the number of defect particles is very small ($N_D \leq 7$) the according sound speed is very close to the lattice without defect particles ($N_D = 0$) in different directions with $C_s(l,0) = 0.868$, $C_s(l,\pi/2) = 0.849$, $C_s(t,0) = 0.132$, and $C_s(t,\pi/2) = 0.116$, showing the anisotropy characteristics of the dust lattice. As the number of defect particles gradually increases, the change of dispersion relation will accordingly cause the change of sound speed. For example, when N_D is 16, although the longitudinal sound speeds are close to those of $N_D = 0$ and 7, while the transverse dispersion relations show two sound speed values, i.e., in addition to the original lower sound speed values (close to those of $N_D = 0$ and 7), the higher

sound speeds appear in two directions with $C_s(t,0) = 0.863$ and $C_s(t,\pi/2) = 0.896$, which are close to those of the longitudinal waves. These indicate the anisotropic property of such a hexagonal dust lattice becomes weaker when the number of defect particles increases to a certain value.

4. Conclusions

The effects of the number of defect particles on the 2D dust lattice structure and dispersion relation are investigated. Particle distribution, the nearest neighbor configuration and pair correlation function are used to show the lattice structure characteristics. The current autocorrelation function, the dispersion relation and sound speed are used to represent the wave properties. It shows that as the increase of the defect particle number, the order of the lattice structure becomes weaker, the current autocorrelation functions and the dispersion relations of the transverse and longitudinal waves in parallel and perpendicular directions show different characteristics. The presence of defect particles has a greater effect on the transverse waves than on the longitudinal waves of the dust lattice. When the number of defect particles increases to a certain value, a higher frequency branch appears in the dispersion relations of the transverse waves. The results of dispersion relation and sound speed show the anisotropy property of such a dust lattice and the appearance of defect particles in the lattice can weaken the anisotropy property of the lattice.

Acknowledgement

Project supported by the National Natural Science Foundation of China (Grant Nos. 12075315 and 11675261).

References

[1] Bonitz M, Filinov V S, Fortov V E, Levashov P R and Fehske H 2005 *Phys. Rev. Lett.* **95** 235006
[2] Yang X F, Wang X G and Liu Y 2009 *Chin. Phys. B* **18** 4938
[3] Farokhi B 2013 *J. Plasma. Phys.* **79** 629
[4] Shahmansouri M and Farokhi B 2012 *J. Plasma. Phys.* **78** 259
[5] Caplan M E 2020 *Phys. Rev. E* **101** 023201
[6] Schella A, Mulsow M, Melzer A, Hählert H, Block D, Ludwig P and Bonitz M 2013 *New. J. Phys.* **15** 113021
[7] Melzer A, Homann A and Piel A 1996 *Phys. Rev. E* **53** 2757
[8] Thomas H M and Morfill G E 1996 *Nature* **379** 806
[9] Melzer A, Schweigert V A, Schweigert I V, Homann A, Peters S and Piel A 1996 *Phys. Rev. E* **54** R46
[10] Sun X X, Wang C H and Wang X G 2007 *Chin. Phys. Lett.* **24** 771
[11] Couëdel L, Zhdanov S K, Ivlev A V, Nosenko V, Thomas H M and Morfill G E 2011 *Phys. Plasmas* **18** 083707
[12] Pieper J B and Goree J 1996 *Phys. Rev. Lett.* **77** 3137
[13] Peters S, Homann A, Melzer A and Piel A 1996 *Phys. Lett. A* **223** 389
[14] Thompson C, Barkan A, Angelo N D' and Merlino R L 1997 *Phys. Plasmas* **4** 2331
[15] Li F and Havnes O 2001 *Phys. Rev. E* **64** 066407
[16] Goree J 1994 *Plasma. Sources. Sci. T* **3** 400
[17] Draine B T and Salpeter E E 1979 *Astrophys. J.* **231** 77
[18] Havnes O, Morfill G E and Goertz C K 1984 *J. Geophys. Res.* **89** 10999
[19] Slattery W L, Doolen G D and DeWitt H E 1980 *Phys. Rev. A* **21** 2087
[20] Ichimaru S 1982 *Rev. Mod. Phys.* **54** 1017
[21] Röcker T, Ivlev A, Zhdanov S and Morfill G 2014 *Phys. Rev. E* **89** 13104
[22] Huang X M, Wang C H and Sun X X 2015 *Journal of Hefei University of Technology (Natural Science)* **38** 569
[23] Morfill G E, Thomas H M, Konopka U M, Rothermel H M, Zuzic M M, Ivlev A M and Goree J M 1999 *Phys. Rev. Lett.* **83** 1598
[24] Quinn T M, Crowley T J and Taylor F 1996 *Geophys. Res. Lett.* **23** 3413
[25] Schmidt P, Zwicknagel G, Reinhard P G and Toepffer C 1997 *Phys. Rev. E* **56** 7310
[26] Ohta H and Hamaguchi S 2000 *Phys. Plasmas* **7** 4506
[27] Ohta H and Hamaguchi S 2000 *Phys. Rev. Lett.* **84** 6026
[28] Liang Z X, Xi D, Zhang Z D and Wu B 2008 *Phys. Rev. A* **78** 023622
[29] Wieben F and Block D 2019 *Phys. Rev. Lett.* **123** 225001
[30] Farokhi B, Kourakis I and Shukla P K 2006 *Phys. Lett. A* **355** 122
[31] Liu Y, Liu B, Chen Y, Yang S Z, Long W and Wang X 2003 *Phys. Rev. E* **67** 066408